Amplification of Electromagnetic Signals by Ion Channels

Juris Galvanovskis and John Sandblom
Department of Medical Biophysics, Göteborg University, 413 90 Göteborg, Sweden

ABSTRACT Cells may respond to the exposure of low-frequency electromagnetic fields with changes in cell division, ion influx, chemical reaction rates, etc. The chain of events leading to such responses is difficult to study, mainly because of extremely small energies associated with low-frequency fields, usually much smaller than the thermal noise level. However, the presence of stochastic systems (for instance, ion channels) provides a basis for signal amplification, and could therefore, despite the low signal-to-noise ratio of the primary response, lead to the transmission of weak signals along the signaling pathways of cells. We have explored this possibility for an ion channel model, and we present a theory, based on the formalism of stochastically driven processes, that relates the time averages of the ion channel currents to the amplitude and frequency of the applied signal. It is concluded from this theory that the signal-to-noise ratio increases with the number of channels, the magnitude of the rate constants, and the frequency response of the intracellular sensing system (for instance, a calcium oscillator). The amplification properties of the stochastic system are further deduced from numerical simulations carried out on the model, which consists of multiple identical two-state channels, and the behavior for different parameters is examined. Numerical estimates of the parameters show that under optimum conditions, even very weak low-frequency electromagnetic signals (<100 Hz and down to 100 μT) may be detected in a cellular system with a large number of ion channels.

INTRODUCTION

Biological systems have been shown to respond to magnetic fields of low intensity and low frequency at the cellular level as well as in biochemical reactions (see, for example, Carpenter and Ayrapetyan, 1994). However, on physical grounds it has been argued that the energy of the fields is much too low relative to the noise inherent in biological systems for the field to produce any observable effects (Schwan, 1985; Weaver and Astumian, 1990; Adair, 1991, 1994). Conclusions like these have mainly been arrived at by considering the physical mechanisms of primary interaction between the magnetic fields and possible biological sites, such as electrical charges in motion, molecules with magnetic moments, or local currents from the generation of electric fields by a varying magnetic field. In all of these cases, the interaction is very weak at field strengths less than 1 mT and frequencies below 1 kHz.

On the other hand, in electronic devices it is quite possible for weak signals, much weaker than the noise level, to be detected in a system as long as the detector bandwidth is narrowly limited around the signal frequency. A signal may also be detected in an inherently noisy system if the system is composed of a series of parallel detectors where the output is a summation of the simultaneous input of the signal into all detectors.

Such amplification mechanisms have not been widely discussed in the context of biological systems, however, and the focus has been rather on possible primary interaction mechanisms that may be specific to biological systems (see, for example, Nordén and Ramel, 1992; Carpenter and Ayrapetyan, 1994).

We have therefore investigated the possibility of amplification of weak electromagnetic signals in cellular systems by considering ion channels whose gating properties are modulated by external fields in a way that has been discussed in connection with the phenomenon of stochastic resonance (McNamara and Wiesenfeld, 1989; Gammaitoni et al., 1989; Zhou and Moss, 1990; Petracchi et al., 1993, 1994; Kruglikov and Dertinger, 1994). Single channel currents are generated by the random switching of channels between open and closed states, and a periodic signal that interacts with the kinetics of each channel will also modulate the total membrane current. The formal theory for such periodically driven stochastic processes has been developed (McNamara and Wiesenfeld, 1989; Jung, 1993) and has been applied to a wide variety of naturally occurring and artificial processes, such as geological phenomena (Benzi et al., 1982; Nicolis, 1982) and neural networks in biology (Longtin et al., 1991; Collins et al., 1995, 1996), and, in electronics, to superconducting quantum interference devices (Hibbs et al., 1995).

We have applied the concepts of such periodically driven stochastic processes to a model consisting of ion channels modulated by a weak sinusoidally varying magnetic field. The model is basically that of McNamara and Wiesenfeld (1989) who developed a theory for a single bistable system modulated by a periodic signal. We have extended the treatment to the case of unequal opening and closing rates and to multichannel systems. Also, in our treatment we have used the approach developed by Jung (1993) for stochastically driven processes, and we have made use of the statistics of multichannel systems (DeFelice, 1981). From the

Received for publication 18 February 1997 and in final form 21 August 1997.

Address reprint requests to Dr. John Sandblom, Department of Medical Biophysics, Göteborg University, Medicinaregatan 11, 413 90 Göteborg, Sweden. Tel.: 46-31-773-3551; Fax: 46-31-773-3558; E-mail: sandblom@clavicula.mednet.gu.se.

0006-3495/97/12/3056/10 $2.00

theory, it is concluded that factors such as the magnitude of the rate constants, the number of channels, and the frequency of the modulating signal will influence the signal-to-noise ratio, and it is shown that a suitable choice of channel parameters can lead to a high degree of signal amplification. We conclude that under optimal conditions these factors can combine to amplify the weak primary response generated by the field to a degree that is sufficiently above the noise level to allow the signal to be detected by a cell.

A presentation of the theory will be given below, and the properties of ion channels as signal detectors will be examined by model simulations.

THEORY

The purpose of the theory is to calculate time averages of the total current $I(t)$ through a set of N channels when the kinetics of opening and closing the channels are synchronously modulated by a sinusoidal signal. This is done by setting up and solving the master equation for the time dependence of the channel states. From the solution to the master equation, it is then possible to calculate averages and power spectra of the channel currents. The procedure follows partly one that has been developed for periodically driven stochastic processes (Jung, 1993), and the first step is to derive expressions that apply to single-channel currents. The treatment is then extended to multichannel systems.

Master equation for a single channel

We proceed from a simple two-state (open-closed) channel, whose open and closed states we designate by O and C, respectively. An applied AC field (electric or magnetic) is assumed to perturb the rate constants for opening and closing (Fig. 1). As shown in the figure, the upward deflection of the AC signal decreases the closing rate and increases the opening rate, and this leads to an increased probability that the channel will be in the open state. The downward deflection creates the opposite effect and leads to an increased probability that the channel will be in the closed state.

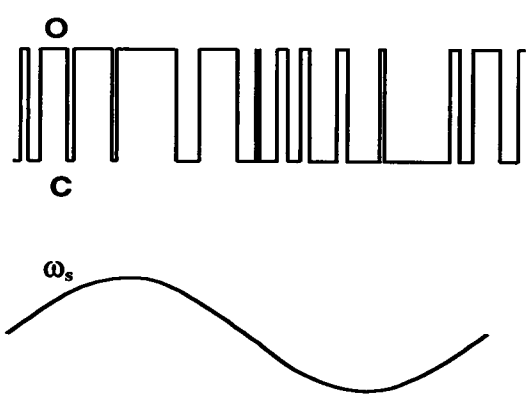

FIGURE 1 The ion current flowing through a single externally modulated ion channel is shown (*top*) together with the modulating signal (*below*). The figure demonstrates, in an exaggerated manner, the modulating effect of the signal on channel dwell times. At the highest signal value the open times are increased and the closed times are diminished; the opposite takes place half a period later. O, Open state; C, closed state; ω_s, angular frequency of the signal.

The rate constants for this system are assumed to be perturbed by a periodic term,

$$k^o(t) = k_0^o e^{\varepsilon^o(t)/kT} = k_0^o(1 + p^o \cos \omega_s t) \tag{1a}$$

$$k^c(t) = k_0^c e^{\varepsilon^c(t)/kT} = k_0^c(1 + p^c \cos \omega_s t) \tag{1b}$$

where k_0^c, k_0^o are the values of the unperturbed rate constants; p^c and p^o are the amplitudes of the modulated parts, assumed to be small so that only the first-order terms need to be retained in the expansion of the exponential functions (Benzi et al., 1982; McNamara and Wiesenfeld, 1989; Jung and Hänggi, 1991; Jung, 1993); and ω_s is the angular frequency of the modulating signal.

Fig. 2 shows the energy profile for the transitions between open and closed states and where the meaning of the kinetic constants is made apparent.

In this simple two-state model, we can write the rate equations for the probabilities $n^o(t)$ and $n^c(t)$ that the channel is either open or closed, the so-called master equations, as

$$\begin{aligned} \frac{dn^o(t)}{dt} &= -k^o(t)n^o(t) + k^c(t)n^c(t) \\ \frac{dn^c(t)}{dt} &= -k^c(t)n^c(t) + k^o(t)n^o(t) \end{aligned} \tag{2}$$

To solve these equations, we introduce, for convenience and shortness of notation, the following constants:

$$K^+ = k_0^o + k_0^c \tag{3a}$$

$$K^- = k_0^o - k_0^c$$

$$K_p^+ = k_0^o p^o + k_0^c p^c \tag{3b}$$

$$K_p^- = k_0^o p^o - k_0^c p^c$$

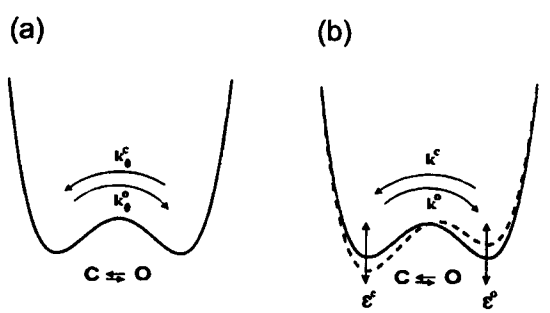

FIGURE 2 The energy profile for the transitions between open (O) and closed (C) states in an unmodulated (*a*) and in a modulated (*b*) channel. The figure shows the meaning of the kinetic constants. k_0^o, k_0^c, Unperturbed rate constants; ε^o, ε^c, modulating signals for open and closed states, correspondingly.

We also take into account that $n^o(t) + n^c(t) = 1$, and combine Eqs. 2 and 3 to get

$$\frac{dN(t)}{dt} = -(K^+ + K_p^+ \cos \omega_s t)N(t) + K \tag{4}$$

where $N(t)$ and K are defined as

$$N(t) = n^o(t) - n^c(t) + \frac{K_p^-}{K_p^+} \tag{5a}$$

$$K = \frac{K^+K_p^- - K^-K_p^+}{K_p^+} = \frac{(p^o - p^c)}{2} \cdot \frac{((K^+)^2 - (K^-)^2)}{K_p^+} \tag{5b}$$

$n^o(t)$ and $n^c(t)$ can then be obtained from $N(t)$ by

$$n^o(t) = \frac{1}{2}\left[1 - \frac{K_p^-}{K_p^+} + N(t)\right] \tag{6a}$$

$$n^c(t) = \frac{1}{2}\left[1 + \frac{K_p^-}{K_p^+} - N(t)\right] \tag{6b}$$

To solve for $N(t)$, we note that Eq. 4 is a linear differential equation with a periodic coefficient, and such an equation can be solved explicitly in terms of modified Bessel functions of the first kind I_ν, as will be shown below.

Solution to the master equation

The formal solution to Eq. 4 is straightforward and is given by

$$N(t) = N(t_0)e^{f(t_0)-f(t)} + Ke^{-f(t)} \int_{t_0}^{t} e^{f(t)}dt \tag{7}$$

where

$$f(t) = \int [k^o(t) + k^c(t)]dt = K^+t + \frac{K_p^+}{\omega_s} \sin \omega_s t \tag{8}$$

The integral in Eq. 7 can be split into two parts:

$$\int_{t_0}^{t} e^{f(t)}dt = \int_{-\infty}^{t} e^{f(t)}dt - \int_{-\infty}^{t_0} e^{f(t)}dt \tag{9}$$

and, by substitutions, $\tau = t - t'$ in the first integral, and $\tau' = t_0 - t'$ in the second integral. Eq. 7 reads

$$N(t) = e^{f(t_0)-f(t)}\left[N(t_0) - K\int_0^\infty e^{f(t_0-\tau')-f(t_0)}d\tau'\right] + K\int_0^\infty e^{f(t-\tau)-f(t)}d\tau \tag{10}$$

where the functions f are given by Eq. 8, with respective arguments.

$N(t)$ is seen from this equation to be composed of two terms, the first of which is a decaying oscillatory function in t. The second term, which describes a quasistationary state, is periodic, with a period of $T_s = 1/2\pi\omega_s$. This stationary periodic part of $N(t)$, given by the last term in Eq. 10, will be denoted by $N_s(t)$ and will be used later to compute the stationary variances and power spectrum of the channel current.

The exponential terms in Eq. 10 can be expanded in Bessel functions with the help of the following formula:

$$e^{a \cos x} = \sum_{-\infty}^{\infty} I_\nu(a) \cos \nu x \tag{11}$$

where I_ν are modified Bessel functions of the first kind. After some algebraic manipulations, we get

$$N_s(t) = K\int_0^\infty e^{f(t-\tau)-f(t)}d\tau = K\int_0^\infty e^{-K^+\tau + (K_p^+/\omega_s)[\sin \omega_s(t-\tau) - \sin \omega_s t]}d\tau$$

$$= K\int_0^\infty e^{-K^+\tau} \sum_{-\infty}^{\infty} I_\nu\left(-K_p^+ \frac{\sin(\omega_s/2)\tau}{\omega_s/2}\right)\cos \nu\omega_s\left(t - \frac{\tau}{2}\right)d\tau \tag{12}$$

The function $N_s(t)$ is seen to form a Fourier series in t:

$$N_s(t) = \sum_{-\infty}^{\infty} c_\nu e^{i\nu\omega_s t} \tag{13a}$$

where, taking into account that $I_\nu = I_{-\nu}$, the coefficients c_ν can be written

$$c_\nu = K\int_0^\infty e^{-K^+\tau} I_\nu\left(-K_p^+ \frac{\sin(\omega_s/2)\tau}{\omega_s/2}\right)e^{-i\nu\omega_s(\tau/2)}d\tau \tag{13ba}$$

The absolute values of c_ν are therefore given by

$$|c_\nu|^2 = K^2\int_0^\infty\int_0^\infty e^{-K^+(\tau'+\tau'')} I_\nu\left(-K_p^+ \frac{\sin(\omega_s/2)\tau'}{\omega_s/2}\right) I_\nu\left(-K_p^+ \frac{\sin(\omega_s/2)\tau''}{\omega_s/2}\right)\cos\left(\nu\omega_s \frac{\tau' - \tau''}{2}\right)d\tau'\, d\tau'' \tag{14}$$

The integrand in this expression consists of an exponential decaying term multiplied by Bessel functions with oscillating arguments and by a cosine function. The signal amplitude p enters into the arguments of the Bessel functions as part of K_p^+ (see Eq. 3b). For the function $N_s(t)$ (Eqs. 13), we can now compute the power spectra of the channel current, using the formalism of stochastically driven processes.

Power spectra of channel currents

Jung (1993) has shown that the power spectrum of a periodically driven stochastic process contains delta peaks at multiples of the modulating frequency, and the weights of these delta peaks are the Fourier coefficients of the quasistationary ensemble average of the dynamic variable. Because, in our case, the dynamic variable is the current that has two values 0 and i, the quasistationary ensemble average is equal to $i \cdot n^o(t)_s$. The contribution to the ion current power spectrum $P_s(\omega)$ (energy/angular frequency) by the modulating signal is therefore given by

$$P_s(\omega) = \frac{i^2}{4} \sum_{-\infty}^{\infty} |c_\nu|^2 \delta(\omega - \nu\omega_s), \qquad \nu \neq 0 \tag{15}$$

where the coefficients $|c_\nu|^2$ are given by Eq. 14. The number 4 in the denominator appears because the open channel probability, apart from a constant, is only one-half of $N_s(t)$ (see Eq. 6a). Because the Bessel functions are symmetrical ($I_\nu = I_{-\nu}$), Eq. 15 can also be written in terms of positive frequencies only:

$$P_s(\omega) = \frac{i^2}{2} \sum_{1}^{\infty} |c_\nu|^2 \delta(\omega - \nu\omega_s) \tag{16}$$

These peaks in the power spectrum of the channel current originate from a superposition of a periodic signal on a stochastic process. This is an interesting result, which demonstrates the essential nonlinearity of the system, that leads to the appearance of the higher harmonics in the resulting power spectrum of the stochastic system, although the imposed signal has only a single frequency. However, these additional peaks in the power spectrum are of the second order or higher and are not discussed in more detail in this article.

Power spectra of multichannel systems

We now extend the treatment to a system of N identical channels of the type described above. Each channel can be in the closed or open state. The current through an open channel has the value i.

If k channels are open at a given instant of time t, the total current $I(t)$ at that instant is given by

$$I(t) = ki \tag{17}$$

where $I(t)$ is a stochastic variable. The probability $P(k)$ that k channels are open in a set of N channels is given by (DeFelice, 1981)

$$P(k) = \frac{N!}{k!(N-k)!} (n^o)^k (n^c)^{N-k} \tag{18}$$

We have also assumed that the applied periodic signal acts synchronously on all channels, which means that $n^o(t)$ and $n^c(t)$ are the same for all channels. The quasistationary mean and variance of $I(t)$ are then given by

$$\text{mean} \quad \langle I(t)_s \rangle = \sum_{k=1}^{N} kP(k) = Nin^o(t)_s \tag{19a}$$

variance

$$\langle I^2(t)_s \rangle = \sum_{k=1}^{N} k^2 P(k) = Ni^2 n^o(t)_s n^c(t)_s + N^2 i^2 (n^o(t)_s)^2 \tag{19b}$$

Because $I(t)$ is the dynamic variable for the multichannel case, it follows from Eq. 19a and the theory of Jung (1993) that the power spectral component $P_s(\omega)$ originating from the periodic signal is given by the Fourier expansion of $n^o(t)_s$ multiplied by $(Ni)^2/2$:

$$P_s(\omega) = \frac{(Ni)^2}{2} \sum_{1}^{\infty} |c_\nu|^2 \delta(\omega - \nu\omega_s) \tag{20}$$

We will now compare the signal power expressed by Eq. 20 with the noise generated by channel fluctuations.

Channel noise

The Lorentzian part of the total power spectrum of the channel current is calculated from the quasistationary averages (Eq. 19). However, because Eq. 19 contains periodic functions, it is necessary to perform a phase averaging of these quasistationary functions over an entire period,

$$\langle I(t)_s \rangle_t = Ni \frac{1}{T_s} \int_0^{T_s} n^o(t)_s dt \tag{21a}$$

and

$$\langle I^2(t)_s \rangle_t = Ni^2 \frac{1}{T_s} \int_0^{T_s} n^o(t)_s n^c(t)_s dt + N^2 i^2 \frac{1}{T_s} \int_0^{T_s} (n^o(t)_s)^2 dt \tag{21b}$$

To integrate these expressions, we will use the Fourier expansions of $n^o(t)_s$ and $n^c(t)_s$

$$n^o(t)_s = \frac{1}{2} \left[1 - \frac{K_p^-}{K_p^+} + \sum_{-\infty}^{\infty} c_\nu e^{i\omega_s t} \right] \tag{22a}$$

$$n^c(t)_s = \frac{1}{2} \left[1 + \frac{K_p^-}{K_p^+} - \sum_{-\infty}^{\infty} c_\nu e^{i\omega_s t} \right] \tag{22b}$$

where c_ν are given by Eq. 13b.

Then the mean value of the current reads

$$\langle I(t)_s \rangle_t = Ni \frac{1}{2} \left[1 - \frac{K_p^-}{K_p^+} + c_0 \right] \tag{23}$$

To evaluate the variance, we first calculate the second term in Eq. 21b:

$$N^2 i^2 \frac{1}{T_s}\int_0^{T_s} (n^o(t)_s)^2 dt = \frac{1}{4}(Ni)^2\left(\left[1 - \frac{K_p^-}{K_p^+} + c_0\right]\right)^2 + \frac{1}{2}(Ni)^2 \sum_1^\infty |c_\nu|^2 \quad (24)$$

It is seen that this term consists of the square of the mean current and the total power of the periodical part of the current. Therefore, the first term in Eq. 21b must express the total noise power generated by the stochastic process. We calculate this term in a similar way to get

$$Ni^2 \frac{1}{T_s}\int_0^{T_s} n^o(t)_s n^c(t)_s dt = Ni^2\left[\frac{1}{4}\left(1 - \left(\frac{K_p^-}{K_p^+} - c_0\right)^2\right) - \frac{1}{2}\sum_1^\infty |c_\nu|^2\right] \quad (25)$$

In summary, therefore, the second term of Eq. 24 gives the total power of the periodic current component and Eq. 25 gives the total noise power. By division, we get the signal-to-noise ratio (SNR):

$$\text{SNR} = \frac{N\Sigma_1^\infty |c_\nu|^2}{\frac{1}{2}(1 - (K_p^-/K_p^+ - c_0)^2) - \Sigma_1^\infty |c_\nu|^2} \quad (26a)$$

If instead of powers, we use amplitudes, Eq. 26a can be rewritten as

$$\frac{\text{signal amplitude}}{\text{noise amplitude}} = \frac{\sqrt{N\Sigma_1^\infty |c_\nu|^2}}{\sqrt{\frac{1}{2}(1 - (K_p^-/K_p^+ - c_0{}^2 - \Sigma_1^\infty |c_\nu|^2}} \quad (26b)$$

$|c_\nu|^2$ in Eq. 26 are obtained from Eq. 14. Two special cases of interest simplify the signal-to-noise ratio.

$\omega_s \ll K^+$

The exponential term in Eq. 14 decays rapidly for large values of K^+ in this case and contributes to the integral only as long as $\omega_s \tau \ll 1$. Equation 14 then reduces to

$$|c_\nu|^2 = K^2\left[\int_0^\infty e^{-K^+\tau} I_\nu(-K_p^+\tau) d\tau\right]^2 = \frac{K^2}{K^{+2} - K_p^{+2}}\left[\frac{K^+ - \sqrt{(K^+)^2 - (K_p^+)^2}}{K_p^+}\right]^{2\nu} \quad (27)$$

If, in addition, the value of p is very small, Eq. 27 reduces further to

$$|c_\nu|^2 = \frac{K^2}{(K^+)^2}\left[\frac{K_p^+}{2K^+}\right]^{2\nu} \quad (28)$$

It is seen from this expression that the higher order terms in ν decrease faster with smaller p values than the lower order terms. Therefore, the signal-to-noise ratio for small p becomes

$$\text{SNR} = \frac{N}{8}\frac{(p^o - p^c)^2((K^+)^2 - (K^-)^2)}{(K^+)^2} \quad (29)$$

$K_p^+ \ll \omega_s$

Because in this case the Bessel functions decrease rapidly for higher values of ν, we calculate only the first term ($\nu = 1$) in Eq. 14. We further expand the Bessel functions in power series of the argument and retain only the first term. Equation 14 for $\nu = 1$ then reduces to

$$\begin{aligned} |c_1|^2 &= K^2 \int_0^\infty \int_0^\infty e^{-K^+(\tau' + \tau'')}\left(-K_p^+ \frac{\sin \omega_s/2\,\tau'}{\omega_s}\right) \cdot \left(-K_p^+ \frac{\sin \omega_s/2\,\tau''}{\omega_s}\right)\cos \omega_s\left(\frac{\tau' - \tau''}{2}\right) d\tau'\, d\tau'' \\ &= \left(\frac{K}{2K^+}\right)^2 \frac{K_p^{+2}}{\omega_s^2 + K^{+2}} \\ &= \frac{(K^+K_p^- - K^-K_p^+)^2}{(2K^+)^2(\omega_s^2 + K^{+2})} \\ &= \left(\frac{p^o - p^c}{2}\right)^2 \frac{((K^+)^2 - (K^-)^2)^2}{(2K^+)^2(\omega_s^2 + (K^+)^2)} \end{aligned} \quad (30)$$

The signal-to-noise ratio in this case is therefore given by a formula,

$$\text{SNR} = \frac{N}{8}\frac{(p^o - p^c)^2((K^+)^2 - (K^-)^2)}{(K^+)^2 + \omega_s^2} \quad (31)$$

Numerical simulations

The properties of the model described in the previous section can be shown by carrying out numerical simulations on a system of identical two-state channels. The starting point is to create a simple simulation process that allows one to obtain the time course of events for a bistable system (in this case a single-channel current recording in real time) performing transitions between two states.

To create a simulation process for this model, we consider a system in which switching between the closed and open states of a channel is a purely random simple Poisson process driven only by noise. The residence times in this case are exponentially distributed. The average residence (dwell) time $\bar{\tau}$ in the corresponding state is equal to the

inverse transition rate k for leaving it. Then, to generate a set of lifetime values for a particular simulation experiment, the source equation can be written as

$$\frac{\tau_k}{\bar{\tau}} = -\ln(\mathrm{RND}) \tag{32}$$

where RND is a random number chosen uniformly inside the interval 0 to 1; τ_k ($k = 1, 2, \ldots, n$) are the consequtive residence times in a given state. Equation 32 allows us to calculate a set of residence times in closed and open states and thus to generate the time course of the ionic current through the channel for a given experiment.

The time-dependent channel potential profile is periodic and $\bar{\tau}$ is therefore also a function of time. For this reason, Eq. 32 must be extended to yield the consecutive τ_k values for the periodically modulated channel potential. We do this by introducing a periodic term in the equation relating the transition rate or the inverse average residence time to the activation energy ΔU:

$$k = \frac{1}{\bar{\tau}} = \nu e^{-(\Delta U/kT)} \tag{33}$$

where ν is the oscillation frequency of the gate inside the channel complex and kT is the thermal noise acting on it. In the presence of a periodic driving force, the activation energy changes as

$$U = \Delta U_0 + \epsilon(t) \tag{34}$$

where ΔU_0 is the activation energy without driving and $\epsilon(t)$ is the forcing function. For convenience, we split the average residence times of the channel states into two parts, $\bar{\tau}_0$ corresponding to the stationary potential, and another part, which incorporates the periodically modulated potential profile:

$$\frac{1}{\bar{\tau}} = \nu e^{-(\Delta U_0 + \epsilon(t)/kT)} = \frac{1}{\bar{\tau}_0} e^{\epsilon(t)/kT} = \frac{1 + p\cos\omega_s t}{\bar{\tau}_0} \tag{35}$$

Combining Eqs. 32 and 35 yields the length of residence times in the presence of the driving signal:

$$\tau_k^{c,o} = -\frac{\bar{\tau}_0^{c,o}\ln(\mathrm{RND})}{1 + p^{c,o}\cos\omega_s t} \tag{36}$$

where $\tau_k^{c,o}$ are random residence times for closed and open states, respectively; $\bar{\tau}_0^{c,o}$ are nonmodulated parts of the average residence times in closed and open states; and $p^{c,o}$ are the modulation amplitudes for the respective rates.

Numerical simulations were performed in MATLAB. At first, the series of closed and open time intervals were calculated according to Eq. 36. Subsequently, a single-channel current recording in real time was obtained by sampling this series at a sampling time smaller than the characteristic period of the channel. The obtained data, containing approximately half a million points in a routine simulation experiment, were split into overlapping sections (the overlap rate was half the section length) of 16,384 points; the Hanning window was applied to each data section. Numerical simulations were performed at rather high p values ($p \approx 0.5$) to make the discussed effects more visible.

Fig. 3 *A* is a plot of the power spectral density as a function of frequency for simulated time series data with the channel dwell times calculated according to Eq. 36, and with equal transition rates from open to closed and closed to open states (symmetrical case). The power spectrum consists of two parts. One part is the broadband noise, which is a characteristic Lorentzian distribution, and the other part is the signal output, which is represented by a peak at a frequency of the external modulating signal. As can be seen, the signal strength increases with the amplitude of modulating signal (Fig. 3 *B*) and decreases when the signal frequency is increased (Fig. 3 *C*). The signal strength found by numerical simulations (*filled circles*) is in good agreement with the predictions (*line*) of Eq. 30.

The simple algorithm we used to calculate the dwell times is very fast, and it gives good results for values of $p <$ 0.8 and for modulation frequencies less than the cut-off frequency of the system simulated. At p values close to unity and signal frequencies considerably higher than the cut-off frequency, too many channel transitions are missed. This leads to a rapid decrease of a signal power for time series data calculated at high signal frequencies (Fig. 3 *C*).

An interesting observation from the theoretical derivation is the appearance of higher harmonics of the modulating signal in the power spectrum of the stochastic system when the potential profile is asymmetrical, even if the signal itself has only a single frequency component. This is illustrated by simulations in Fig. 4. Taking the ratio $\bar{\tau}^o/\bar{\tau}^c = 10$ and $p =$ 0.6, the simulated time data series for $\omega_s = 10$ has in its power spectrum at least three clearly visible peaks. The peaks obtained from simulations agree well with the values calculated according to Eq. 27.

Fig. 5 illustrates the theoretical prediction that the signal-to-noise ratio increases when the channel transition rates increase (Eq. 31). The reason for this effect is twofold—first, the total noise power does not depend on the magnitude of the transition rates, and, second, the higher transition rates lead to an increased dispersion of the Lorentzian part of the power spectrum. These two effects in combination cause lowering of the noise floor, which enhances the signal-to-noise ratio.

The amplification of an external signal brought about by an increase in the number of synchronously modulated channels is seen from the simulation results shown in Fig. 6. For two channels (Fig. 6 *B*) operating synchronously, the signal amplitude is twice as big as for a single channel (Fig. 6 *A*).

DISCUSSION

We have shown in this investigation, by numerical simulations and by theoretical analysis, that a coherent modulation of ion channel gating by an external signal leads to the

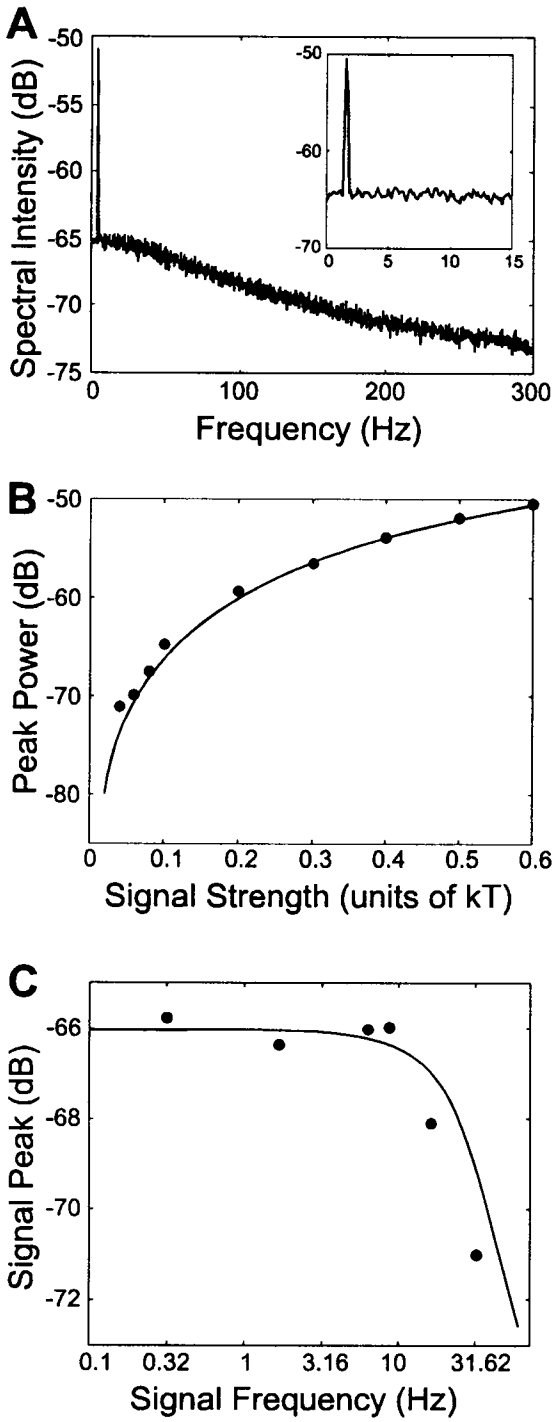

FIGURE 3 (*A*) A characteristic power spectrum from simulated time series data for a single channel with symmetrical modulation. The parameters are $p^o = p^c = 0.6$, $\tau^o = \tau^c = 0.005$, and $\omega_s = 10$. *Inset*: The low frequency part of the same power spectrum is shown to make the signal peak visible. (*B*) The simulated output power magnitude for the signal (●) as a function of the modulation amplitude. The solid line represents a theoretically expected signal power computed from Eq. 18. The parameters are $\tau^o = \tau^c = 0.01$ and $\omega_s = 10.3544$, and the current i through an open channel is 0.02. The signal frequency is centered on one of the bins to avoid the division of signal power among several bins. (*C*) Experimental (●) and theoretical (————) dependence of signal power on the modulating frequency. The parameters are $\tau^o = \tau^c = 0.01$ and $p^o = p^c = 0.1$, and the current through an open channel is 0.02.

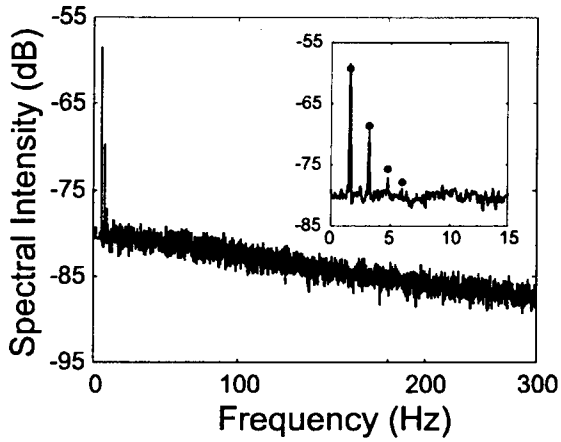

FIGURE 4 The figure shows the appearance of higher harmonics in the transformed signal. The power spectrum from simulated time series data is shown for an asymmetrical single channel modulated with a symmetrical signal. The parameter values are $p^o = p^c = 0.6$, $\tau^o = 0.01$, $\tau^c = 0.001$, and $\omega_s = 10$. *Inset*: The low-frequency part of the same power spectrum is shown to make visible the signal peak and its harmonics. Filled circles correspond to theoretically calculated peak amplitudes (Eq. 15).

occurrence of a periodic component in the ion current across a membrane containing a system of multiple channels. We have also shown that the amplification of the signal power depends on the number of channels and the magnitude of rate constants. However, the response of the cell to the modulated component of the channel current and, consequently, any possible biological consequences will also depend on the presence and sensitivity of a cellular detector for this signal.

The periodic or oscillating intracellular biochemical processes (for instance, a cytosolic calcium oscillator that has been demonstrated in many cell types; Fewtrell, 1994) are the most probable candidates for the role of the signal "detector." Such a "detector" may be assumed to have a very narrow bandwidth $\Delta\omega$, which should be introduced into Eq. 31 to describe the oscillator's response to changes in ion influx caused by both the external signal and random fluctuations.

This can be done by noting that the Lorentzian noise of a two-state channel system decays inversely proportionally to $(K^+)^2 + \omega^2$ (*DeFelice*, 1981). *For a system of N* identical two-state channels, the total noise power within a small frequency interval $\Delta\omega$ is equal to

$$P(\omega)\Delta\omega = \frac{Ni^2}{2\pi}\frac{K^+((K^+)^2 - (K^-)^2)}{(K^+)^2 + \omega^2}\Delta\omega \qquad (37)$$

where we have assumed that the contribution to the total noise of the periodic signal is small ($|p^o|, |p^c| \ll 1$). If we assume that the interval $\Delta\omega$ is centered around ω_s and divide the noise power within $\Delta\omega$ by the total noise power $\int_0^\infty P(\omega)d\omega$, we get from Eq. 37 the fraction of the total noise power F, which is transmitted to the oscillator:

$$F = \frac{\text{noise power within } \Delta\omega}{\text{total noise power}} = \frac{2}{\pi}\frac{K^+\Delta\omega}{(K^+)^2 + \omega_s^2} \qquad (38)$$

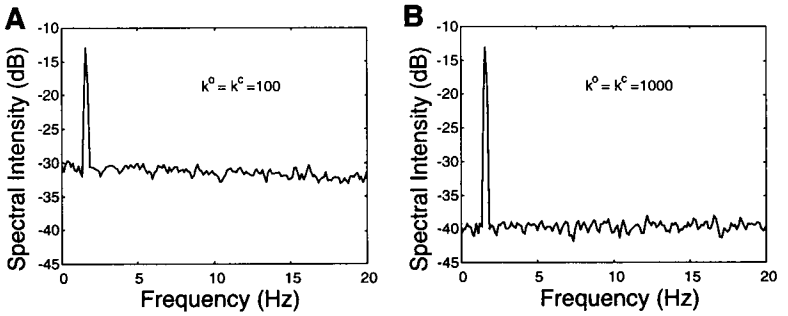

FIGURE 5 The dependence of the signal-to-noise ratio on the channel transition rates. (*A*) The transition rates are $k^o = k^c = 100$. (*B*) $k^o = k^c = 1000$. The modulating signal frequency in both cases is $\omega_s = 10$ and $p^o = p^c = 0.6$. In case (*B*) the noise floor is seen to be considerably lowered because of the increased transition rates. This lowering enhances the signal level over the noise level.

The signal-to-noise ratio at the detector level is then

$$\mathrm{SNR}(\Delta\omega) = \frac{\text{signal power}}{F \times \text{total noise power}} \tag{39}$$

Therefore we get, by dividing Eq. 31 by Eq. 38,

$$\mathrm{SNR}(\Delta\omega) = N\frac{\pi Q}{\omega_s}\frac{p^2(k_0^o k_0^c)}{k_0^o + k_0^c} \tag{40a}$$

or

$$\frac{\text{signal amplitude}}{\text{noise amplitude}} = p\sqrt{N\frac{\pi Q}{\omega_s}}\sqrt{\frac{k_0^o k_0^c}{k_0^o + k_0^c}} \tag{40b}$$

where $p = (p^o - p^c)/2$ and Q is the quality factor $(\omega_s/\Delta\omega)$ of the biochemical oscillator.

Equation 40 brings together in two simple formulas all parameters that determine the amplification of the external electromagnetic signal by a system of N identical ion channels. As has been already mentioned above, these parameters are of two essentially different types. One part, namely, N, p, k_0^o, and k_0^c, characterize physical properties of ion channels that define the power of the periodic component of the ion current across a cell membrane. The other part, the quality factor Q, is the only parameter that, within this model, describes the coupling and response of cell metabolism to the external influence. The coupling parameter Q will determine the possible, if any, occurrence and size of the biological effects.

Equation 40 can also be expressed in terms of average open times τ^o and average closed times τ^c, which are simply the inverse of the corresponding rate constants. This gives a particularly simple expression for the ratio of signal and noise amplitudes:

$$\frac{\text{signal amplitude}}{\text{noise amplitude}} = p\sqrt{N\frac{Q}{2f_s}}\frac{1}{\sqrt{\tau^o + \tau^c}} \tag{41}$$

where the signal frequency f_s is used instead of the angular frequency. Equation 41 is seen to contain the signal-to-noise ratio of the initial absorption process, multiplied by an amplification factor that has been calculated assuming the equality between the signal frequency and the characteristic frequency of an intracellular detector. An estimate of the magnitude of amplification will be made in the following section.

Estimate of the signal amplification in a channel system

To assess the magnitude of amplification of an external electromagnetic signal that is capable of modulating channel gating, we consider a membrane with N voltage-gated channels and a biochemical oscillator (calcium oscillator), which we assume to be the detector of the modulated ion current.

To get an estimate of the signal amplitude, we compute the electric field E induced across the ion channel complex by a 50-Hz alternating magnetic field of amplitude $B = 100$ μT. This follows from the integral form of Faraday's law:

$$\oint_l E \cdot dl = \frac{d(\int_S B \cdot ds)}{dt} = \frac{d\Phi}{dt} \tag{42}$$

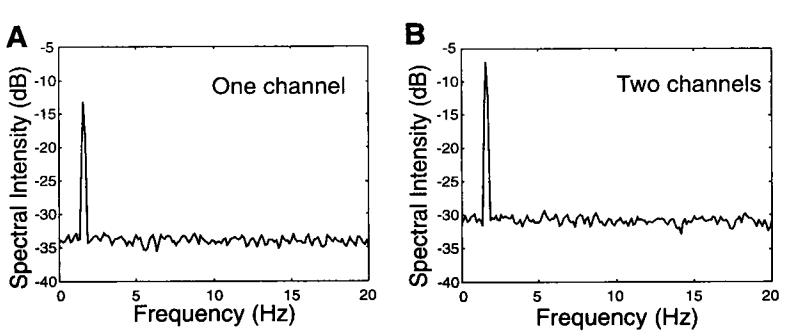

FIGURE 6 The linear increase of the signal power with the number of synchronously modulated channels in the system. (*A*) A single channel. (*B*) Two channels. The parameter values are $p^o = p^c = 0.6$, $\tau^o = \tau^c = 0.005$, and $\omega_s = 10$. Note that the power spectrum magnitude is shown in dB.

where S is an area through which the field B passes, creating a magnetic flux Φ, and l is a path bounding the area S. Then the mean amplitude of the induced electric field $\bar{E}_B$ across a channel that sits in the membrane of a spherical cell with a radius $r_c = 10$ μm is

$$\bar{E}_B = \frac{B\omega r}{2} \cdot \frac{1.5 r_c}{d} \tag{43}$$

where ω is the angular frequency and r is the radius of the area S. The factor $1.5r_c/d$, where d is membrane thickness, corrects for the increase in the field intensity caused by the high resistivity of a membrane relative to the tissue electrolyte. Then, assuming $r = 10$ cm (the radius of the cross section of a human body), Eq. 43 yields $\bar{E}_B \approx 2.5$ V/m, and the induced potential difference between two opposite points on a channel $V_{ind} = \bar{E}_B \cdot d$ is $\sim 2.5 \times 10^{-5}$ mV.

This potential difference synchronously modulates all N voltage-gated channels present in the membrane. As a result of this modulation, the external electromagnetic signal is transformed into a periodic component in the ion current across the membrane. This component, according to the proposed mechanism, acts as a perturbing factor of the Ca oscillator. The ratio between amplitudes of this perturbing signal and noise follows from Eq. 41.

The magnitude of the signal amplitude p in Eq. 41 is then computed as a maximum energy uptake in units of kT of the gating charge of the channel. Taking a channel gating charge $q = 10e$, we obtain $p = q \cdot V_{ind}/kT \approx 10^{-5}$.

Besides the signal amplitude p and the channel number N, the amplification depends on average open and closed times, and the quality factor Q of the biochemical (calcium) oscillator. Because most types of ion channels exhibit burst-like appearances, we assume in order to explore the proposed mechanism under optimal conditions that the average open and closed times are in the μsec range, that is $\tau^o = \tau^c = 10^{-6}$ sec (Colquhoun and Hawkes, 1995).

The quality factor Q can be estimated roughly from results given in the literature. Several frequency dependent biological effects of the weak electromagnetic fields have been detected such as the dependence of the motility of a marine diatom *Amphora coffeaeformis* on exposure to certain combinations of alternating and direct current magnetic fields (McLeod et al., 1987; Smith et al., 1987; Reece et al., 1989). The maximum estimate of Q from these data is 80. That allows us to assume, for the purpose of this estimation, that under optimal conditions $Q = 100$.

Finally, to estimate the number of channels N, we first note that the occurrence of a periodic component in the ion current across a cell membrane is a first-order effect, and will be canceled out by averaging the induced electrical field over a cell surface. It means that symmetrical cells that have ion channels evenly distributed on their surface will not be able to register any changes in the net ion influx under the exposure to the external electromagnetic field. Nevertheless, the mechanism described above will be valid for cells that contain so-called hot spots, i.e., regions with high concentration of ion channels. Several cell types have been demonstrated to possess such regions of high ion channel concentration, for instance, neurons (synapses), B-cells from the pancreas (Bokvist et al., 1995), and others (Kasai et al., 1993; Thorn et al., 1993). The channel molecule densities in specific areas of membranes of excitable cells are very high (up to several thousands per square μm), which justifies the approximation of 1000 channels. Although in membranes of nonexcitable cells the density of channel molecules is considerably lower, it has been demonstrated experimentally for pancreatic B-cells that the number of channels found in "hot spots" may be close to a thousand (Bokvist et al., 1995). The same is true for many types of asymmetrical or vectorial cells, for example, enterocytes of intestinal epithelium, the functional organization of which is such as to create a unidirectional flow of nutrients across the intestinal wall.

Inserting the estimated values in Eq. 41 finally gives

$$\frac{\text{signal amplitude}}{\text{noise amplitude}} = p\sqrt{N\frac{Q}{2f_s}}\,\frac{1}{\sqrt{\tau_o + \tau_c}} \approx 0.3 \tag{44}$$

Although this is still a small value, it shows that the amplification is large enough to bring the signal into the range of detection by a sufficiently efficient detector.

We do not discuss within this investigation the possible net accumulation of ions under the exposure to the harmonic electromagnetic field, since this is a second-order effect (Astumian et al., 1995). However, in our treatment the accumulation of ions can be conveniently derived by analyzing the higher order terms in c_0 (Eq. 14), because c_0 gives the contribution from the modulating signal to the constant part of the ion flux, i.e., it describes the rectification of a time varying signal in a system of ion channels.

An additional possibility for amplification, not contained in our treatment, is the mixing of the applied signal with the external random noise component, which, by the mechanism of stochastic resonance, can enhance the detection limits of cells responding to the external electromagnetic fields (Bezrukov and Vodyanoy, 1997).

In summary, we have focused in this study on the primary mechanisms that a biological cell can use to amplify weak external influences, for instance, an alternating magnetic field. Such amplification mechanisms have tended to be overlooked in attempts to explain the response of cells exposed to electromagnetic fields. We have shown that a system of identical ion channels embedded in a membrane and synchronously modulated can significantly amplify the original signal. The amplification of the signal amplitude relative to the noise amplitude is proportional to the square root of the number of channels modulated and inversely proportional to the square root of the sum of the average channel dwell times. For the external influence to be biologically important, the capability of a cell to detect periodic changes in ionic influx is essential. The cytosolic Ca^{2+} oscillator, a complex system of biochemical reactions that allows a cell to create sophisticated spatiotemporal patterns

of Ca^{2+} intracellular concentration, may function as a detector of the small periodic component of Ca influx.

This work was supported in part by grants from the Swedish Medical Research Council (grant 4138), the Swedish Work Environment Fund, and Jubileumsklinikens Forskningsfond.

REFERENCES

Adair, R. K. 1991. Constraints on biological effects of weak extremely low-frequency electromagnetic fields. *Phys. Rev. A.* 43:1039–1048.

Adair, R. K. 1994. Constraints of thermal noise on the effects of weak 60-Hz magnetic fields acting on biological magnetite. *Proc. Natl. Acad. Sci. USA.* 91:2925–2929.

Astumian, R. D., J. C. Weaver, and R. K. Adair. 1995. Rectification and signal averaging of weak electric fields by biological cells. *Proc. Natl. Acad. Sci. USA.* 92:3740–3743.

Benzi, R., G. Parsi, A. Sutera, and A. Vulpiani. 1982. Stochastic resonance in climatic change. *Tellus.* 34:10–16.

Bezrukov, S. M., and I. Vodyanoy. 1997. Stochastic resonance in non-dynamical systems without response threshholds. *Nature.* 385:319–321.

Bokvist, K., L. Eliasson, C. Ämmälä, E. Renström, and P. Rorsman. 1995. Co-localization of L-type Ca^{2+} channels and insulin-containing secrotory granules and its significance for the initiation of exocytosis in mouse pancreatic B-cells. *EMBO J.* 14:50–57.

Carpenter, D. O., and S. Ayrapetyan, editors. 1994. Biological Effects of Electric and Magnetic Fields, Vol. 1, Sources and Mechanisms; Vol. 2, Beneficial and Harmful Effects. Academic Press, New York.

Collins, J. J., C. C. Chow, and T. T. Imhoff. 1995. Stochastic resonance without tuning. *Nature.* 376:236–238.

Collins, J. J., T. T. Imhoff, and P. Grigg. 1996. Noise-enhanced information transmission in rat SA1 cutaneous mechanoreceptors via aperiodic stochastic resonance. *J. Neurophysiol.* 76:642–645.

Colquhoun, D., and A. G. Hawkes. 1995. The principles of the stochastic interpretation of ion-channel mechanisms. *In* Single-Channel Recordings, B. Sakman and E. Neher, editors. Plenum Press, New York and London. 397–482.

DeFelice, L. J. 1981. Introduction to Membrane Noise. Plenum Press, New York.

Fewtrell, C. 1994. Ca^{2+} oscillations in non-excitable cells. *Annul Rev. Physiol.* 55:427–454.

Gammaitoni, L., F. Marchesoni, E. Menichella-Saetta, and S. Santucci. 1989. Stochastic resonance in bistable systems. *Phys. Rev. Lett.* 62: 349–352.

Hibbs, A. D., A. L. Singsaas, E. W. Jacobs, A. R. Bulsara, and J. J. Bekkedahl. 1995. Stochastic resonance in a superconducting loop with a Josephson junction. *J. Appl. Phys.* 77:2582–2590.

Jung, P. 1993. Periodically driven stochastic systems. *Phys. Rep.* (*Phys. Lett.*). 234:175–295.

Jung, P., and P. Hänggi. 1991. Amplification of small signals via stochastic resonance. *Phys. Rev. A.* 44:8032–8042.

Kasai, H., Y. X. Li, and Y. Miyashita. 1993. Subcellular distribution of Ca^{2+} release channels underlying Ca^{2+} waves and oscillations in exocrine pancreas. *Cell.* 74:669–677.

Kruglikov, I. L., and H. Dertinger. 1994. Stochastic resonance as a possible mechanism of amplification of weak electric signals in living cells. *Bioelectromagnetics.* 15:539–547.

Longtin, A., A. Bulsara, and F. Moss. 1991. Time-interval sequences in bistable systems and the noise-induced transmission of information by sensory neurons. *Phys. Rev. Lett.* 67:656–659.

McLeod, B. R., S. D. Smith, and A. R. Liboff. 1987. Calcium and potassium cyclotron resonance curves and harmonisc in diatoms (*A. coffeaformis*). *J. Bioelectr.* 6:153–168.

McNamara, B., and K. Wiesenfeld. 1989. Theory of stochastic resonance. *Phys. Rev. A.* 39:4854–4868.

Nicolis, C. 1982. Stochastic aspects of climatic transitions—response to a periodic forcing. *Tellus.* 34:1–9.

Nordén, B., and C. Ramel, editors. 1992. Interaction Mechanisms of Low-Level Electromagnetic Fields in Living Systems. Oxford Science Publications, Oxford.

Petracchi, D., C. Ascoli, M. Barbi, S. Chillemi, M. Pellegrini, and M. Pellegrino. 1993. Periodic forcing of ion channel gating: an experimental approach. *J. Statist. Phys.* 70:393–401.

Petracchi, D., M. Pellegrini, M. Pellegrino, M. Barbi, and F. Moss. 1994. Periodic forcing of a K^+ channel at various temperatures. *Biophys. J.* 66:1844–1852.

Reece, J. A., M. E. Frazier, J. E. Morris, and D. L. Miller. 1989. A confirmation of diatom mobility at 16-Hz electromagnetic fields. Eleventh Annual Bioelectromagnetics Society Meeting, Tucson, Arizona, 18–22 June.

Schwan, H. P. 1985. Biophysical principles of the interaction of ELF-fields with living matter. II. Coupling considerations and forces. *In* Biological Effects and Dosimetry of Static and ELF Electromagnetic Fields, Vol. 19. M. Grandolfo, S. M. Michaelson, and A. Rindi, editors. Plenum Press, New York. 243–271.

Smith, S. D., B. R. McLeod, A. R. Liboff, and K. Cooksey. 1987. Calcium cyclotron resonance and diatom motility. *Bioelectromagnetics.* 8: 215–227.

Thorn, P., A. M. Lawrie, P. Smith, D. V. Gallacher, and O. H. Petersen. 1993. Local and global cytosolic Ca^{2+} oscillations in exocrine cells evoked by agonists and inositol triphosphate. *Cell.* 74:661–668.

Weaver, J. C., and D. Astumian. 1990. The response of living cells to very weak electric fields: the thermal noise limit. *Science.* 247:459–462.

Zhou, T., and F. Moss. 1990. Escape-time distributions of a periodically modulated bistable system with noise. *Phys. Rev. A.* 42:3161–3169.